Spatial Structure and Activity Mechanism of a Novel Spider Antimicrobial Peptide[†,‡]

Peter V. Dubovskii, Pavel E. Volynsky, Anton A. Polyansky, Vladimir V. Chupin, Roman G. Efremov, and Alexander S. Arseniev*

Shemyakin-Ovchinnikov Institute of Bioorganic Chemistry, 16/10 Miklukho Maklaya str., Moscow, 117997 Russia

Received March 31, 2006; Revised Manuscript Received July 3, 2006

ABSTRACT: Latarcins (Ltc), linear peptides (ca. 25 amino acid long) isolated from the venom of the *Lachesana tarabaevi* spider, exhibit a broad-spectrum antibacterial activity, most likely acting on the bacterial plasmatic membrane. We study the structure−activity relationships in the series of these compounds. At the first stage, we investigated the spatial structure of one of the peptides, Ltc2a, and its mode of membrane perturbation. This was done by a combination of experimental and theoretical methods. The approach includes (i) structural study of the peptide by CD spectroscopy in phospholipid liposomes and by ^{1}H NMR in detergent micelles, (ii) determination of the effect on the liposomes by a dye leakage fluorescent assay and ^{31}P NMR spectroscopy, (iii) refinement of the NMR-derived spatial structure via Monte Carlo simulations in an implicit water−octanol slab, and (iv) calculation of the molecular hydrophobicity potential. The molecule of Ltc2a was found to consist of two helical regions (residues 3−9 and 13−21) connected via a poorly ordered fragment. The effect of the peptide on the liposomes suggests the carpet mechanism of the membrane deterioration. This is also supported by the analysis of hydrophobic/hydrophilic characteristics of Ltc2a and homologous antimicrobial peptides. These peptides exhibiting a helix−hinge−helix structural motif are characterized by a distinct and feebly marked amphiphilicity of their N- and C-terminal helices, respectively, and by a hydrophobicity gradient along the peptide chain. The approach we suggested may be useful in studying not only other latarcins but also a wider class of membrane-active peptides.

Antimicrobial peptides (AMPs)[1] are important components of the innate immune system of most organisms (*1*). Among AMPs the linear antimicrobial peptides (L-AMPs) constitute the most studied group (*2*). Most L-AMPs deteriorate the integrity of bacterial plasma membrane rather than disturb complex intracellular pathways (*3*). These peptides represent a suitable model for the de novo design of medicines against microorganisms that have developed resistance to conventional antibiotics. This is due to a high diversity (∼200 members have currently been described), short lengths (less than ∼50 residues), and a relatively simple spatial structure (mainly α-helical in membranes).

Structure−activity studies of L-AMPs revealed that their antimicrobial activity is determined by a number of molecular properties such as positive charge, α-helicity, and amphipathy (*4*). Several sequence-based parameters (e.g., degree of amphipathy, mean hydrophobicity, and charge distribution) were used to differentiate L-AMPs (*2*, *4*−*7*), but unambiguous sequence−activity relationships are yet to be disclosed. A low predictive power of the sequence-based methods is determined by a simplified description of the hydrophobic characteristics of amino acid residues, because each of them is assigned with only a single value (e.g., hydrophobicity index). Obviously, highly heterogeneous hydrophobic/hydrophilic organization of amino acid residues along with their location in the spatial structure of an L-AMP under study should be taken into account. This could be done using the molecular hydrophobicity potential (MHP) method (*8*). The formalism of MHP utilizes a set of atomic physicochemical parameters evaluated from octanol−water partition coefficients (log *P*) of numerous chemical compounds. It permits the detailed assessment and pictorial visualization of the molecular hydrophobic/hydrophilic properties. This method has earlier been successfully applied to mapping of the spatial polarity properties and for the determination of the membrane binding mode for a number of peptides and proteins (*9*, *10*). Implications of the MHP approach to L-AMPs could permit

[†] This work was supported by the Russian Foundation for Basic Research, project numbers 02-04-48882a, 04-04-48875a, and 06-04-49588a, Program MCB of the Russian Academy of Sciences, Federal Agency for Science and Innovations (State Contract 02.46711.3003 of April 20, 2005; Grant SS-1522, 2003). R.G.E. is grateful to the Russian Science Support Foundation for the grant awarded.

[‡] NMR constraints and derived atomic coordinates of the peptide in detergent micelles (20 models) have been deposited with the Protein Data Bank (accession code 2G9P).

* Corresponding author: telephone, (495) 330-5929; e-mail, aars@nmr.ru; fax, (495) 335-5033.

[1] Abbreviations: 2D, two dimensional; 3D, three dimensional; AMP, antimicrobial peptide; L-AMP, linear antimicrobial peptide; CBF, carboxyfluorescein; CD, circular dichroism; CSA, chemical shift anisotropy; Cec-Mag, hybrid cecropin−magainin peptide; DOPE, dioleoylphosphatidylethanolamine; DOPG, dioleoylphosphatidylglycerol; DrsB2, dermaseptin B2; L/P, lipid to peptide molar ratio; LUV, large unilamellar vesicles; Ltc2a, latarcin 2a; MD, molecular dynamics; MC, Monte Carlo method; MHP, molecular hydrophobicity potential; NMR, nuclear magnetic resonance; NOESY, 2D nuclear Overhauser effect spectroscopy; PE, phosphatidylethanolamine; PG, phosphatidylglycerol; RMSD, root-mean-square deviation; SDS, sodium dodecyl sulfate; SDS-d_{25}, deuterated sodium dodecyl sulfate; TOCSY, 2D total correlated spectroscopy; ppm, parts per million.

10.1021/bi060635w CCC: $33.50
Published on Web 08/04/2006

the delineation of specific patterns on a peptide surface and, on the basis of the hydrophobic match/mismatch concept, the prediction of the mode of membrane binding and the putative mechanism of action. Evidently, the accuracy of such conclusions depends on the availability of information on the spatial structure of AMPs in the membrane.

Nuclear magnetic resonance (NMR) spectroscopy is known to be an excellent technique for the elucidation of spatial structures of peptides incorporated in the membrane-mimicking environment (*11*, *12*). However, such experiments often provide information only on peptide conformation, while the molecular details of peptide−membrane interactions are lost. Also, often ill-ordered peptide fragments lack a sufficient number of NMR constraints, and as a result, the quality of the spatial structure suffers. A possible solution to these problems may consist in an additional structure relaxation and refinement via computer simulations in implicit or explicit membrane mimics using the available NMR constraints. The peptide molecular dynamics (MD) in explicit membrane environments (full-atom hydrated lipid bilayers or micelles) or membrane mimics seems to be one of the most powerful techniques for this purpose (*13*). Unfortunately, this method requires extensive computer calculations and has to be used with care in cases when the peptide location in the membrane is unknown. A reliable compromise between preserving atomic details and the computational cost of simulations appears to be an employment of Monte Carlo (MC) conformational search in an implicit membrane model. This approach has been successfully applied previously to exploration of the membrane binding mode of a number of peptides and proteins (*14*).

Elucidation of the molecular mechanisms of membrane-perturbing activity of L-AMPs is the next important step in structure−activity studies of AMPs. Most L-AMPs primarily act on plasmatic membrane of bacteria (*3*), and hence, the mechanism of their membrane perturbation can be studied on model phospholipid membranes (*4*, *15*). Most conveniently, this can be achieved by experimental methods using nonperturbing membrane probes and nuclei, in particular, ^{31}P NMR spectroscopy (*16*−*20*).

Thus, the molecular mechanisms of L-AMP action can be understood using a combined approach with the use of the aforementioned experimental and theoretical techniques. We have implemented such an approach for a number of peptides recently isolated from the venom of the spider *Lachesana tarabaevi* (*21*). One of the most interesting of them is the Ltc2a peptide, a quite hemolytic 26 aa cationic peptide with activity against Gram-positive and Gram-negative bacteria. The goal of this work is the determination of its spatial structure in the membrane-bound state and the mechanism of its membrane-perturbing action. We determined the spatial structure of Ltc2a by high-resolution NMR spectroscopy in sodium dodecyl sulfate (SDS) micelles and then refined it via MC calculations in the implicit water−octanol slab. We used a mixture of phosphatidylethanolamine (PE) and phosphatidylglycerol (PG) to adequately model the lipid composition of bacterial plasmatic membranes (*22*). The membrane-bound structure of Ltc2a and the effect of this peptide on PE−PG liposomes were determined by circular dichroism (CD) spectroscopy, dye leakage fluorescent measurements, and ^{31}P NMR spectroscopy. Our results provide a new insight into the functionality of this L-AMP when supplemented with information on its antibacterial activity (*21*).

MATERIALS AND METHODS

Materials. Deuterated SDS (SDS-d_{25}) was obtained from Cambridge Isotope Laboratories. Dioleoylphosphatidylethanolamine (DOPE) and dioleoylphosphatidylglycerol (DOPG), polycarbonate membranes of pore diameter either 100 or 400 nm, were supplied by Avanti Polar Lipids (Alabaster, AL). Carboxyfluorescein (CBF), SDS, and Sephadex G-50 were products of Sigma-Aldrich (St. Louis, MO). ^2H_2O (99.9%) was purchased from ISOTOPE (Russian Federation). The pH of aqueous solutions of the peptides or peptide/detergent mixtures was adjusted with diluted KOH or HCl (REACHIM, Russian Federation).

Sample Preparation. Ltc2a was synthesized by Fmoc methodology. A sample for studying Ltc2a in SDS micellar solution was obtained by a stepwise addition of SDS-d_{25} (from 200 mM stock solution in a 9:1 $H_2O-{}^2H_2O$ mixture) at pH 6.8 to the aqueous solution (2.5 mg/500 μL of 9:1 $H_2O-{}^2H_2O$) of the peptide until the SDS-d_{25}:peptide molar ratio has reached the value of ∼60:1. The sample in ^2H_2O was prepared by lyophilization of the sample in H_2O (Ltc2a−SDS-d_{25}, 1:60) at pH 6.8, followed by redissolution in ^2H_2O.

Liposomes composed of the DOPE−DOPG (molar ratio 7:3) mixture were prepared by mixing the required amounts of the phospholipids dissolved in chloroform and evaporation on a Savant Speedvac vacuum dryer, model SPD1010 (GMI, Inc., Albertville, MN). The resulting film was overnight dried at a high vacuum and then hydrated with 50 mM Tris-HCl buffer prepared in $H_2O-{}^2H_2O$ (50:50 v/v) containing 100 mM KCl. A freeze−thawing was performed to facilitate soaking of the film. The phospholipid dispersion was extruded through a polycarbonate filter with a pore size of 400 nm. Freshly prepared and size-calibrated unilamellar vesicles (LUVs) in the buffer (total lipid of 6 mg/240 μL) were placed in an NMR tube with an outer diameter of 5 mm. The peptide dissolved in the same buffer was added to the liposomes in 5 μL portions, and the tube was shaken to facilitate homogenization of the sample.

NMR Spectroscopy. ^{1}H NMR spectra (NOESY and TOCSY) for structure elucidation were measured on a Varian Unity-600 spectrometer equipped with a triple resonance probe, an actively shielded *z*-gradient coil, and a current amplifier, PERFORMA II. The details of the measurements and processing of the data were the same as reported in ref *23*.

The ^{31}P NMR spectra were recorded on a Bruker Avance spectrometer (DRX 500) at the resonance frequency of 202.5 MHz, using a standard broad-band 5 mm probe head. Chemical shifts were referenced relative to an external 85% H_3PO_4. The spectra were recorded with the $S = {}^1/_2$ Hahn echo pulse sequence. A recycle delay of 2.5 s was used. A total number of 2048 accumulations (accumulation time of ∼1.5 h) was acquired. All of the measurements were carried out at 10 °C. The spectra were processed using Bruker XWINNMR software as earlier described (*24*). The lineshape simulation of the spectra was achieved with the program P-FIT under an assumption that the lines are purely Lorentzian and the liposomes adopt an ellipsoidal shape in the magnetic field (*25*). The adjustable parameters in the

simulation protocol were the components of the tensor of chemical shift anisotropy (CSA), the integral intensity, the semiaxis ratio of the ellipsoid, and the half-width of Lorentzian band.

Spatial Structure Calculation and Analysis. The program CYANA (*26*) was used for the calculation of the structure of Ltc2a bound to SDS micelles. At the first step, the volumes of NOE cross-peaks were calibrated using the standard subroutine CALIBA (*27*). After a preliminary structure was obtained, the NOEs were calibrated by a systematic comparison of NOE volumes with proton−proton distances in the set of calculated structures. The torsion angle restraints were obtained with a local structure analysis using the HABAS program (*27*), based on $d_{N\alpha}(i,i)$, $d_{N\beta}(i,i)$, and $d_{\alpha N}(i,i+1)$ NOE constraints in NOESY spectra with a short mixing time (60 ms). No ^3J proton−proton coupling constants were used in the analysis, because their measurements were hampered by relatively broad line widths in the ^{1}H NMR spectra. Local structure analysis also resulted in the identification of unambiguous stereospecific assignments whose number was increased on further stages of spatial structure calculation. NOE and angle restraints were supplemented with data on the deuterium exchange rates of amide protons. Slowly exchanging amides of residues 6−8 and 19 were supposed to participate in hydrogen bonding. The most probable carbonyl acceptors for these amides were selected in the preliminary structure calculation without any restraints for hydrogen bonds. As a result, at least in 50% of calculated structures the carbonyl groups of residues 2−4 and 15 were hydrogen bonded with the amide groups from residues 6−8 and 19, respectively. The restraints amounting to respective i, $i + 4$ hydrogen bonds were added.

A macro ANNEAL utilizing MD in torsion angle space was used for the structure calculation (*26*). The standard MD protocol with a stepwise decrease in the temperature comprised of 10000 steps was employed. A set of 200 random structures was minimized, and 20 of them with minimal target function were selected. They were used for the analysis of violated distance constraints and refinement of stereospecific assignment with the GLOMSA utility (*27*). Visualization and analysis of the calculated structures were achieved with the MOLMOL (version 2.2) (*28*) and PROCHECK (vesrion 3.4.4) programs (*29*, *30*).

Molecular Modeling. Twenty structures with low violations of NMR constraints were the starting conformations of Ltc2a for MC simulations. The membrane was represented by an effective potential based on a combined employment of atomic solvation parameters for gas to octanol and gas to water transfer, which mimic the lipid−water interface and the aqueous solution, respectively (*31*). The details of the implicit membrane model are given in ref *14*. Conformational space of proteins was explored via a variable temperature MC search in the space of torsion angles using the modified FANTOM program (*32*). The starting structures were arbitrarily placed in the aqueous phase. Then several consecutive MC runs for each starting conformation with applied NMR restraints were carried out as described earlier (*10*). The resulting lowest energy structures were analyzed using a set of specially written auxiliary programs. Several parameters, such as the peptide location in the membrane slab, angles between axes of helices, and the bilayer normal, were monitored. Hydrophobic properties of α-helices were calculated and visualized using the MHP approach as described in ref *8*.

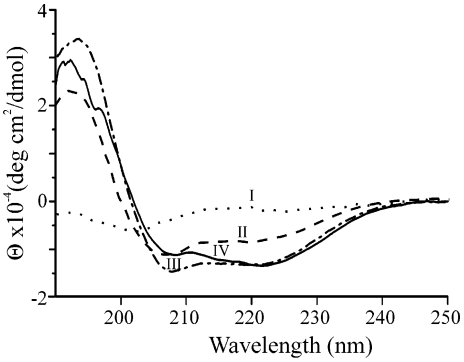

FIGURE 1: CD spectra of Ltc2a in various environments: (I) at 18 °C, pH 6.8, 0.6 mM in water (dotted line); (II) 0.3 mM in water−TFE (50:50 v/v) (dashed line); (III) 0.25 mM in SDS micelles (SDS−peptide, 100:1) (dot−dashed line); (IV) 0.23 mM in DOPE−DOPG (7:3) LUV (diameter of 100 nm), L/P, 77:1 (solid line).

CD Spectroscopy. CD spectra were measured on a JASCO-810 spectropolarimeter. All of the spectra were obtained at room temperature with a quartz cell of 0.1 mm path length. The concentration of the peptide varied from 0.2 to 1.4 mM. The baseline-corrected spectra were smoothed, and the helical content was estimated as previously described (*33*).

Leakage Experiments. Lipid film (DOPE−DOPG, 7:3) was hydrated with 50 mM Tris-HCl buffer containing 100 mM KCl and 50 mM CBF. The lipid dispersions were subjected to as many as 10 freeze−thaw cycles and subsequently extruded through a polycarbonate filter with a pore size of 100 nm. Nontrapped CBF was removed by gel filtration on a Sephadex G-50 column equilibrated with 50 mM Tris-HCl buffer, pH 7.5, containing 100 mM KCl. These vesicles were then diluted to a final volume of 1.2 mL with the same buffer (total lipid concentration of ∼20 μM), and the release of CBF after addition of the peptide was monitored by measuring fluorescence intensity at 515 nm with excitation at 492 nm on a Hitachi F-4000 instrument at room temperature. The release of CBF was calculated according to the equation:

$$R_f = 100[(F_t - F_0)/(F_{100} - F_0)]$$

where R_f is the fraction of the dye released, F_0, F_t, and F_{100} are the fluorescence intensities at times $t = 0$ (i.e., prior to the peptide addition), t (∼2 min after the peptide addition accompanied by sample stirring), or after addition of 10 μL of 10% Triton X-100 solution, respectively.

RESULTS

Spatial Structure of Ltc2a. CD spectra of Ltc2a in various environments are shown in Figure 1. The spectrum in the aqueous solution (pH 6.8) is a typical one of the random coil state. Similar spectra were obtained within the pH range from 2.5 to 7.5. A helical conformation emerges in membranelike environments, in water−TFE mixture, in SDS micellar solution, and in the presence of DOPE−DOPG (7:3) phospholipid vesicles. The helical content was estimated to reach up to 40% for the SDS solution. The CD spectrum of the peptide in the presence of PE−PG vesicles is similar

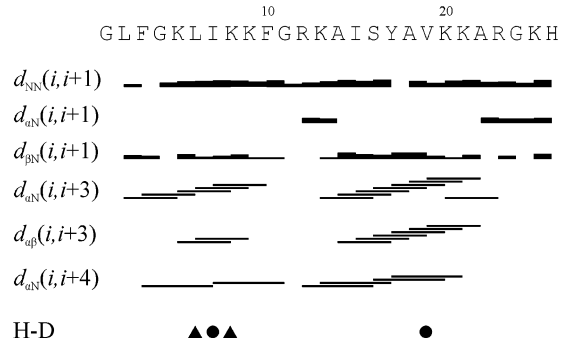

FIGURE 2: $^1H-^1H$ contacts from 60 ms NOESY spectra of Ltc2a−SDS (1:60) at pH 6.8, 45 °C, and H−D exchange rates of amide protons. The widths of the bars correspond to the relative volume of the corresponding cross-peaks in the NOESY spectrum. The amides that persisted in the spectra for >10 h (Ile7 and Val19) are designated with filled circles. The filled triangles correspond to the amides with a lifetime of ~5 h (Leu6 and Lys8). The volumes of cross-peaks overlapped under the conditions were evaluated from NOESY spectra measured at slightly different temperature or pH.

to that in SDS micelles (Figure 1), indicating similarity of the peptide structure in bilayers and micelles.

Ltc2a exhibits narrow ^1H NMR resonance lines in aqueous solution (spectra not shown). An addition of SDS-d_{25} results in line broadening, which indicates an interaction of the positively charged peptide with the negatively charged micelles. An SDS to peptide molar ratio of 60:1 was used to keep approximately one peptide molecule per micelle (*34*). A temperature of 45 °C was used to obtain narrower resonance lines. The procedure of the sequential resonance assignments was applied straightforwardly (*35*). An analysis of the α-proton chemical shifts of the peptide revealed their upfield shifts, indicating the formation of α-helical structure (*36*, *37*). NOE connectivities for Ltc2a in SDS micelles are shown in Figure 2. A number of d_{NN}, $d_{\alpha N}(i,i+3)$, $d_{\alpha\beta}(i,i+3)$, $d_{\alpha N}(i,i+4)$ connectivities imply that the peptide adopts α-helical structure within residues 3−9 and 13−21 connected with an unordered fragment (residues 10−12).

In total, 222 distance and 123 torsion angle constraints were used for the structure calculation. No long-range NOEs were detected. This might indicate that no peptide−peptide association takes place under the conditions used. The statistics of the NMR set are provided in Table 1. MC refinement of the NMR structure in the implicit membrane allowed to improve the Ramachandran statistics with a minimal effect on the peptide structure (Table 1).

A set of 20 structures of Ltc2a with lowest violations of the input distance constraints is shown in Figure 3a. The peptide molecule comprised of two α-helices separated by a poorly ordered fragment is shown in a ribbon representation in Figure 3b. A large portion of hydrogen bonds of the Ltc2a molecule are of *i*, *i* + 4 type, where *i* + 4 is the number of residues with the NH group, while the CO group of residue *i* is its acceptor. The following hydrogen bonds are highly populated within the calculated set: Leu6···Leu2, Ile7···Phe3, Lys8···Gly4, Ser16···Arg12, Tyr17···Lys13, Val19···Ile15, Lys20···Ser16, Lys21···Tyr17, and Ala22···Ala18. Only two *i*, *i* + 3 hydrogen bonds are formed: Lys9···Leu6 and Arg23···Lys20. Note that only four hydrogen bonds were assumed in the calculations: Leu6···Leu2, Ile7···Phe3, Lys8···Gly4, and Val19···Ile15, because the corresponding amide protons were slowly exchanging (Figure 2).

Table 1: Structural Statistics for the Final Family of 20 Ltc2A Structures[a]

parameter	value
target function (Å)	0.14 ± 0.01
upper limit violations (Å)	
sum	1.3 ± 0.1
maximum	0.11 ± 0.01
lower limit violations (Å)	
sum	0.0 ± 0.0
maximum	0.00 ± 0.00
van der Waals violations (Å)	
sum	0.3 ± 0.0
maximum	0.11 ± 0.00
violations of torsion angle constraints (deg)	
sum	0.6 ± 0.5
maximum	0.48 ± 0.42
pairwise RMSD (Å)	
backbone, residues 3−21	0.94 ± 0.36 (1.33 ± 0.90)
heavy atoms, residues 3−21	1.77 ± 0.35 (2.01 ± 0.93)
backbone, residues 3−8	0.38 ± 0.20 (0.31 ± 0.25)
heavy atoms, residues 3−8	1.11 ± 0.24 (0.99 ± 0.41)
backbone, residues 13−21	0.22 ± 0.06 (0.07 ± 0.03)
heavy atoms, residues 13−21	1.27 ± 0.40 (0.71 ± 0.30)
Ramachandran statistics[b]	
residues in most favored regions (%)	73.6 (87.6)
residues in additionally allowed regions (%)	22.9 (12.4)
residues in generously allowed regions (%)	2.4 (0)
residues in disallowed regions (%)	1.1 (0)

[a] The values were obtained by calculations using constraints generated from the 60 ms NOESY spectrum of Ltc2a−SDS (1:60), pH 6.8, 45 °C, for 20 of 200 structures calculated and followed by restrained minimization in the implicit model membrane (values in parentheses). [b] Analyzed using PROCHECK, v.3.4.4 (*29*, *30*).

The two helices of Ltc2a differ in their hydrophobic organization. The N-terminal helix is strongly amphiphilic. The side chains of hydrophobic and hydrophilic amino acids are segregated into the opposed sides (Figure 3c,d). The hydrophobic side of this helix is formed by the Phe3, Leu6, and Ile7 residues. The opposed hydrophilic side is built up of the side chains of residues Lys5, Lys8, and Lys9. The N-terminal hydrophobic residues and Phe10 of the hinge region constitute a hydrophobic site, which could be inserted in the lipid bilayer. On the other hand, the hydrophobic (Ile15, Tyr17, and Val19) and hydrophilic (Lys13, Lys20, Arg12, and Ser16) residues are randomly distributed on the surface of the C-terminal helix.

We used MC simulation to putatively localize the peptide molecule in the lipid bilayer. The positioning of the best structure of the final set in the water−octanol slab is shown in Figure 3b. The consideration of the whole set of structures showed that the N-terminal helix should be buried in the membrane at an angle of 55 ± 15° relative to the membrane plane. The apolar residues of this helix display energetically favorable contacts with the membrane environment in good accord with the hydrophobic match−mismatch concept. Unfavorable interactions are observed only for the Lys5 residue due to the immersion of its side chain in the hydrophobic medium. The C-terminal helix lies nearly parallel to the slab (angle between the helix axis and the membrane plane is −15 ± 12°) and slightly interacts with the water−octanol interface.

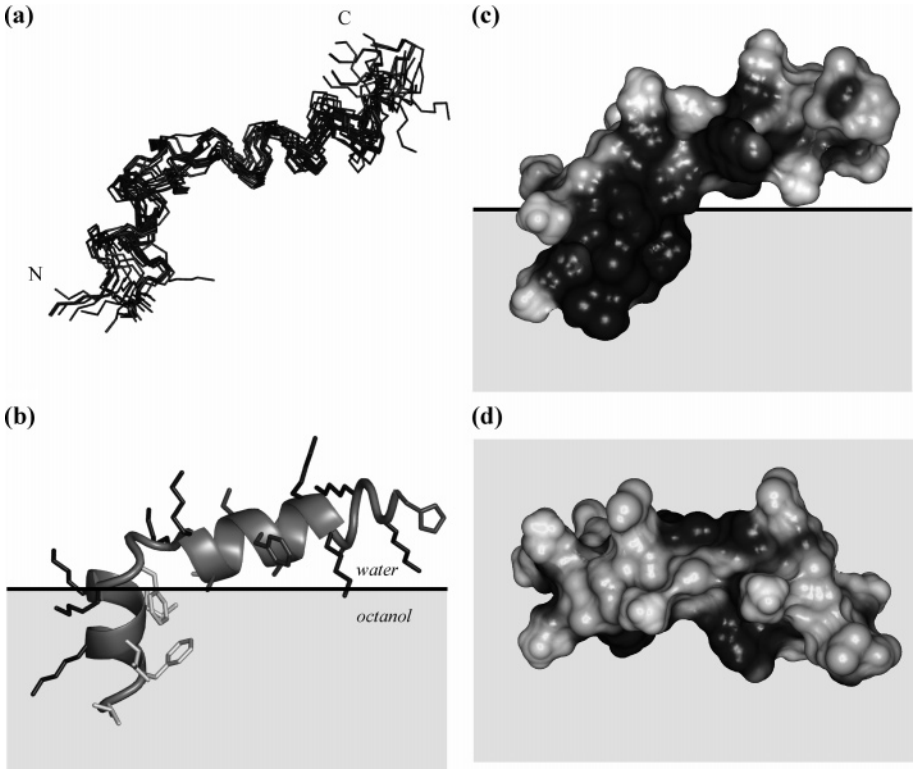

FIGURE 3: Structure of Ltc2a based on NMR data in SDS micelles and restrained MC simulations in the implicit membrane. Ensemble of 20 representative structures superimposed by backbone atoms of residues 3−21 (a). Membrane binding mode for the best structure (b). The peptide backbone is given as a ribbon representation. Charged, polar, and hydrophobic residues are shown by black, dark gray, and light gray sticks, respectively. Implicit membrane is in hatched gray. Spatial hydrophobic properties (c, d) of the peptide surface: side (c) and top views (d). The peptide surface is colored according to the values of the molecular hydrophobicity potential (MHP) created on the surface points by the atoms of Ltc2a. Hydrophobic (high MHP) and hydrophilic (low MHP) surface regions are shown in dark and light gray, respectively.

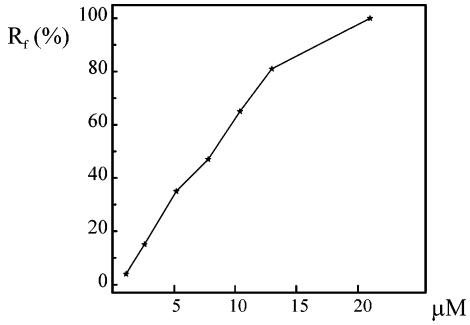

FIGURE 4: Release of CBF from DOPE−DOPG (7:3) LUVs (diameter of 100 nm) at pH 7.5 as a function of peptide concentration.

Interaction of Ltc2a with Liposomes. We studied the interaction of Ltc2a with liposomes formed by a mixture of PE and PG to elucidate a possible mechanism of its antibacterial action. Figure 4 shows the percentage of CBF leakage from DOPE−DOPG (7:3) liposomes as a function of the peptide concentration. The results indicate that Ltc2a interacts with the liposomes and increases the permeability of the lipid bilayer. A ^{31}P NMR study of the Ltc2a interaction with LUVs of the same lipid composition was carried out to understand the membrane permeability mechanism. The liposomes obtained by extrusion through 400 nm pores exhibit a ^{31}P NMR spectrum (Figure 5a) with a typical bilayer line shape. No averaging of CSA due to vesicle tumbling was observed in accordance with earlier observations for the liposomes of a similar size (*38*). The line shape in the spectrum is similar to that observed for PE−PG multilamellar liposomes (*19*). Up to a L/P ratio ≥∼25:1, the bilayer-type shape of the spectrum is preserved. As an example, the ^{31}P NMR spectrum at a L/P ratio of 50:1 is shown in Figure 5b. If the spectra (Figure 5a,b) are fitted with a single axially

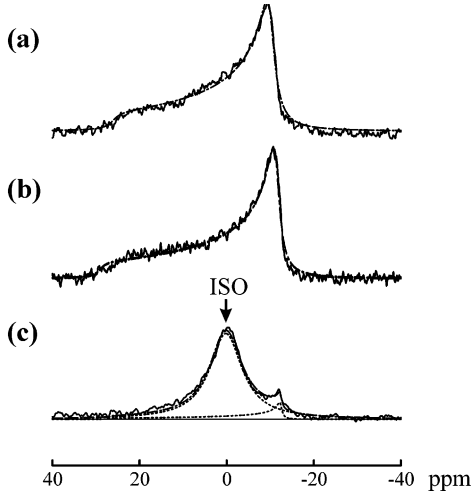

FIGURE 5: ^{31}P NMR spectra of DOPE−DOPG (7:3) liposomes (a) in the absence or (b) in the presence of Ltc2a at L/P ratios of 50:1 and (c) 18:1. The solid lines correspond to the computer- simulated spectra obtained using the program P-FIT (*25*). The dotted lines in (c) correspond to the isotropic and anisotropic components, with the arrow pointing to the isotropic one. The best-fit CSA values (ppm) were (a) 36.2, (b) 39.8, and (c) 39.8. The liposomes were assumed to be ellipsoidal in shape, with the aspect ratio c/a ∼1.15, where c and a are major and minor axes of the ellipsoid, respectively.

symmetric powder pattern, the CSA value is found to be increased from ~36 to 40 ppm. This is in agreement with a complete miscibility of PE−PG mixtures (*39*). At a L/P ratio <~20:1, the peptide was found to destroy the bilayer organization. The ^{31}P spectrum at a L/P ratio of 18:1 is a superposition of two signals, anisotropic and broad isotropic, with the integral intensities in a ratio of 1:9 (Figure 5c). Therefore, it can be concluded that Ltc2a deteriorates the phospholipid organization when the concentration of the bound peptide exceeds a threshold value.

DISCUSSION

It has recently been found that Ltc2a, a member of a new family of latarcins from the venom of the *L. tarabaevi* spider, possesses cytolytic and antimicrobial activities against both Gram-positive and Gram-negative bacteria, acting presumably on the integrity of plasma membranes (*21*). In this work, we proved the structure of this peptide by CD spectroscopy in membrane- mimicking environments, such as water−TFE mixture, SDS micelles, and phospholipid vesicles. The peptide was shown to exhibit a higher degree of helicity in the micelles than in the water−alcohol mixture. This observation is similar to those made earlier for other membrane peptides (cf. ref *40*). Ltc2a adopts in the micelles and the phospholipid vesicles [DOPE−DOPG (7:3) mixture] structures of a similar overall helicity, and therefore, we have concluded that the detergent micelle is a suitable membrane model. The high-resolution NMR structure of Ltc2a was then solved in the SDS micelle, and this structure was subjected to refinement by MC simulation in the implicit membrane, a water−octanol slab. An advantage of this technique over MD simulations is that it is much faster due to the implicitness of the membrane. In addition, MC search in the dihedral angle space permits exhaustive sampling of the potential energy surface, thus providing efficient localization of the low-energy states of a peptide in the membrane.

The resulting spatial models of Ltc2a are believed to bear a considerable resemblance to its conformation in biological membranes. This is supported not only by the helical content of the peptide detected by CD spectroscopy in liposomes but also by the fact that NMR-derived micelle-bound conformations of a number of amphiphilic α-helical peptides are similar to those in lipid bilayers (*33*, *41*). Furthermore, according to the MC simulation data, the resulting spatial structure of Ltc2a is well adopted to the planar water−octanol slab (see below). The observed helix−hinge−helix structural motif frequently occurs in cationic AMPs. Usually, in the peptides composed of more than ~20 amino acids the helical regions are not continuous but contain a flexible hinge in the middle part. Such segments are often enriched with helix-breaking residues, Gly and/or Pro (*42*). For instance, structure−activity studies revealed the necessity of a hinge in caerin 1.1 (*43*), a synthetic AMP composed of fragments of cecropin, magainin-2 (*42*), and clavanin (*44*). This structural motif is expected to predetermine the mechanism of the peptide action on the bacterial plasma membrane.

Basically, there are two mechanisms by which linear amphipathic AMP permeates bacterial plasma membranes. This occurs either by (a) transmembrane pore formation via a barrel stave or by (b) a carpetlike mechanism (*15*). The first one presumes that no disintegration of the membrane takes place. The peptide molecules bound to the outer membrane leaflet associate themselves in such a way that the hydrophobic peptide regions align with the lipid core region, while the hydrophilic peptide regions form the interior of the pore. The carpet mechanism presumes the peptides disrupt the membrane by covering the surface of the lipid bilayer and forming a monolayer, a carpet. A combination of ^{31}P NMR and fluorescence spectroscopies in this work and also the information on the planar bilayer membranes, obtained recently (*21*), allow us to suggest that Ltc2a likely acts via the carpet mechanism.

Indeed, the ^{31}P NMR suggests that the Ltc2a binding to PE−PG liposomes at low peptide concentrations (Figure 5b) increases the ^{31}P CSA value. This increase agrees with previous studies on the effect of cations on lipid bilayers, showing that the conformation of lipid headgroup changes by moving out of the bilayer surface toward the water phase (*45*). This makes the barrel stave mechanism unlikely, since a peptide must be located near the lipid headgroup under these conditions, as noted by Ramamoorthy and co-workers (*46*). Ltc2a induces formation of the isotropic phase in PE−PG bilayers after a threshold L/P ratio of ~20:1. Disruption of the membranes via observation of a relatively broad isotropic signal in the ^{31}P NMR spectra was evidenced in favor of the carpet mechanism of action of cationic AMP (*47*). Assuming that the peptide is bound only to the outer membrane leaflet, one can calculate that the peptide molecules cover all of the outer surface of the liposomes at a L/P ratio of ~20:1. The liposome breakdown begins exactly under these conditions. We noticed also that at this L/P ratio the leakage of CBF from the liposomes begins (Figure 4). It is likely, that the release of CBF from the liposomes is due to their disruption by Ltc2a and subsequent formation of lipid−peptide complexes. A similar pattern of the interaction was found in a number of studies of peptide−lipid interactions (*24*, *48*, *49*). Note that hydrophobic interactions seem to play a significant role in the formation of these complexes, because the peptide was shown to disrupt zwitterionic and PE−PG planar membranes at similar effective concentrations (*21*).

What might be the relationship between the 3D structure of the micelle-bound Ltc2a and the mechanism of its membrane-perturbing action? To address this issue, a comparative analysis of Ltc2a with other antimicrobials with known properties is required. We tried to find such peptides by searching for the sequence homology in an AMP database (*50*), containing more than 500 entries. Among the identified homologous peptides, only the molecules with the spatial structure resembling that of Ltc2a were considered. As a result, two candidates that meet these criteria were chosen, namely, dermaseptin B2 (DrsB2) and a hybrid cecropin−magainin peptide (Cec-Mag). Both of them reveal a homology degree above 50% with Ltc2a (Figure 6a), and their NMR-derived structures in a membrane mimetic environment exhibit the helix−hinge−helix motif. Despite this fact, the two peptides demonstrate different mechanisms of action. Ceg-Mag forms pores in membranes (*42*), while DrsB2 acts by the carpet mechanism (*51*). This obviously indicates that, based only on the sequence and 3D structure information, it appears impossible to differentiate the peptides according to the membrane-perturbing action. We propose the use of a detailed mapping of hydrophobic−hydrophilic properties

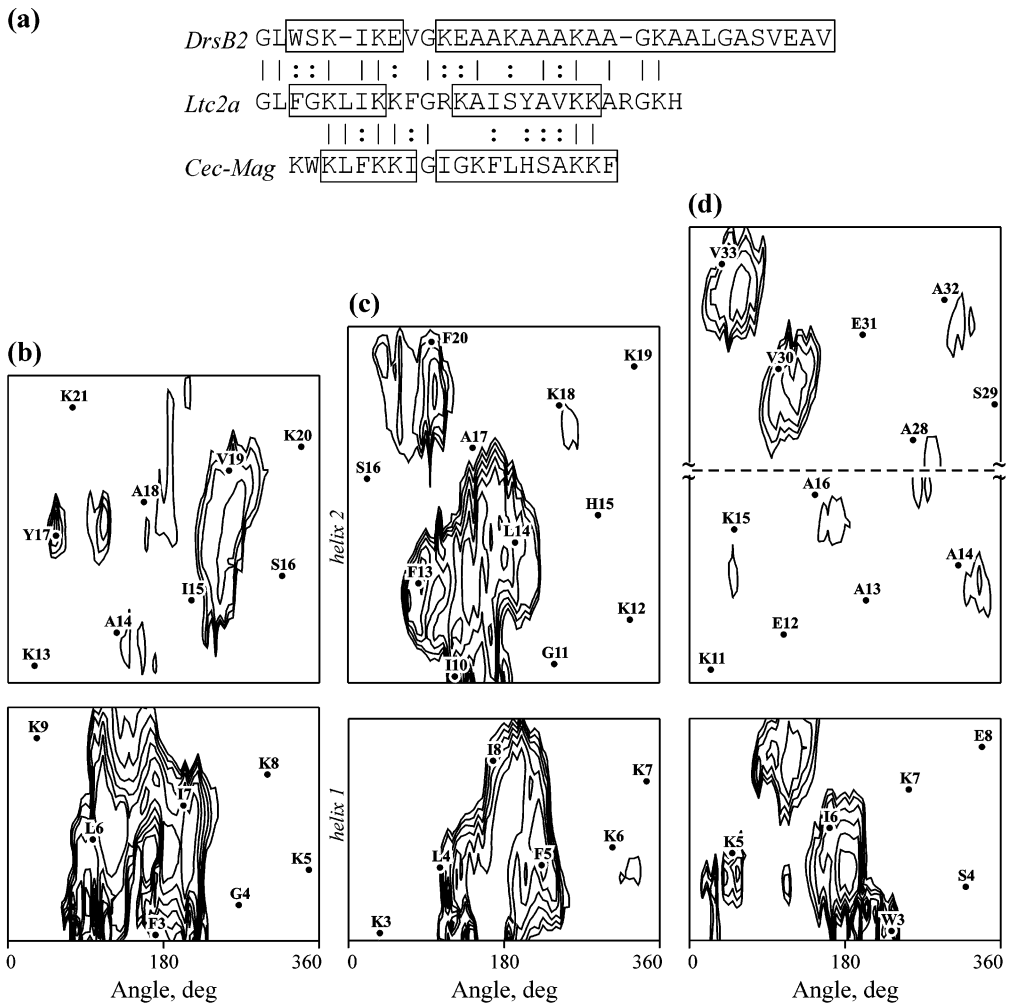

FIGURE 6: Sequence alignment between Ltc2a and structurally similar L-AMPs (a) and hydrophobic organization of Ltc2a (b), Cec-Mag (c), and DrsB2 (d). Identical and isofunctional amino acids in the alignment are marked with the symbols "|" and ":", respectively. Helical regions of the peptides are enclosed in boxes. The 2D isopotential map of the molecular hydrophobicity potential (MHP) on the surface of the peptide helices was calculated as described in ref *8*. The value on the *X* axis is the rotation angle about the helix axis; the parameter on the *Y* axis is the distance along the helix axis. MHP is given in octanol−water log *P* units. Only the hydrophobic areas with MHP > 0.09 are shown. Contour intervals are 0.015. The positions of residues are indicated by letters and numbers. The N- and C-terminal helices of the peptides are given separately on the lower and upper panels, respectively. The nonamphiphilic central region of the second helix of DrsB2 (d) is not shown.

of their α-helical regions using the MHP approach (*8*).

Two-dimensional (2D) MHP maps for α-helices in the NMR models of Ltc2a, Cec-Mag, and DrsB2 are shown in Figure 6b−d. The contour isolines correspond to hydrophobic regions with high positive MHP values on the surfaces of their helices. One can see that the N-terminal helices in all of the peptides are clearly amphiphilic and strongly hydrophobic at one of the helix sides. On the other hand, the C-terminal helices are quite different. For example, such a helix in Ceg-Mag demonstrates a marked amphiphilic character, whereas, in the case of Ltc2a and DrsB2, polar and apolar residues are almost uniformly distributed among the helix sides. Another observation is that the surfaces of the N-terminal helices of Ltc2a and DrsB2 are much more hydrophobic than the C-terminal helices. Such a hydrophobicity gradient (also called as oblique-oriented pattern) was found in many of the so-called tilted peptides (*52*). In contrast, both of the helical segments of Ceg-Mag reveal quite similar hydrophobicities.

It has previously been shown (*53*) that the MHP data for peptides, along with MC simulations in implicit membrane, often help to delineate the mode of membrane binding. For Ltc2a, this is illustrated by an analysis of low-energy states found by MC conformational search in the water−octanol slab. Octanol mimics a weakly polar medium with dielectric properties similar to those on the membrane interfaces. As seen in Figure 3b, a typical energetically favorable conformation of Ltc2a is characterized by an insertion of its N-terminal helix into the slab, while its C-terminal helix resides in the interface. Strong membrane interactions of the former helix are caused by its amphiphilic nature. The Phe3, Leu6, and Ile7 residues forming the hydrophobic pattern on the MHP map contact octanol, while the polar Lys8 and Lys9 residues are exposed to water. The absence of prominent hydrophobic patches on the surface of helix 13−21 impedes its immersion into octanol.

The MHP properties of the membrane-interacting regions of DrsB2 and Ceg-Mag, like those of Ltc2a, correlate with their modes of binding and membrane-perturbing mechanisms. DrsB2 efficiently interacts with the membrane through its amphiphilic N-terminal helix and destabilizes the lipid bilayer in a carpetlike manner. The C-terminal part of DrsB2

was found to be only slightly involved in the membrane binding because of a somewhat diffuse distribution of the hydrophobic properties of its surface. These conclusions agree with the experimental data (*51*, *54*). On the other hand, the membrane-bound motif of Ceg-Mag comprising two amphiphilic helices separated by a flexible hinge is well-suited for the formation of transmembrane pores. This is likely to occur through their assembling into tightly folded α-helical bundles. Such motifs are frequently observed in ion channels (*55*).

To summarize, in this study, we used a combined experimental and theoretical approach to explore the membrane-bound conformation and the mechanism of the membrane-destabilizing action of Ltc2a, a new antimicrobial peptide from the venom of the *L. tarabaevi* spider. We showed that, in the membrane, the Ltc2a molecule consists of two helices separated by a hinge. MC simulations of Ltc2a in a water−octanol slab revealed a peripheral mode of its membrane binding. The results of modeling techniques (MHP and MC) obtained for Ltc2a corroborate the ^{31}P NMR and fluorescence leakage data suggesting the peptide action by the carpet mechanism.

The proposed approach possesses a number of limitations, and some reasonable questions can arise. In particular, the surfaces of bacterial membranes and SDS micelles are negatively charged, while the interface of the model slab is electrically neutral. One might therefore argue that the surface location of the Ltc2a helices may change near the anionic surface. Furthermore, the curvature radii of micelles are much smaller than those of lipid bilayers. In addition, the atomic scale details of the peptide−membrane interactions were not taken into consideration in the MC simulations. How do these factors affect the structure and the binding mode? What structural hydrophobic features of the peptide determine different types of activity against Gram-positive and Gram-negative bacteria and in hemolysis? Last but not least, the relationships between the structure and membrane-perturbing activity proposed in this study for Ltc2a should be validated for other members of the latarcin family and/or some mutants.

We should stress that the membrane perturbation phenomena induced by L-AMPs are much more complex than the models using simplified systems. This is because too many factors determining peptide−membrane interactions have to be properly taken into account. Hopefully, finding specific features of L-AMPs and design of perspective antibiotics with a high therapeutic potential will be facilitated due to a systematic delineation of the relative contributions of such particular factors using independent experimental (NMR and optical spectroscopy) and theoretical (MD simulations in full-atom micelles and lipid bilayers) techniques. To address these issues, we are currently implementing such a combined approach to study other homologous L-AMPs, members of the latarcin family, and their mutants with altered biological activities. The results will be published in due course.

ACKNOWLEDGMENT

We thank Dr. I. A. Kudelina for help with CD measurements, Dr. A. Y. Surovoy for peptide synthesis, and Prof. Y. G. Molotkovsky for granting permission for fluorometer usage. Access to computational facilities of the Joint Supercomputer Center (Moscow) is gratefully acknowledged.

SUPPORTING INFORMATION AVAILABLE

One figure representing deviations of α-proton chemical shifts of Ltc2a in the SDS micelle (1:60) at 45 °C from those in the random coiled state, a plot of the distribution of distance constraints as a function of the residue number difference or residue number, and one figure showing intervals of variation of dihedral angles for the set of calculated structures of Ltc2a. This material is available free of charge via the Internet at http://pubs.acs.org.

REFERENCES

1. Zasloff, M. (2002) Antimicrobial peptides of multicellular organisms, *Nature 415*, 389−395.
2. Dennison, S. R., Wallace, J., Harris, F., and Phoenix, D. A. (2005) Amphiphilic alpha-helical antimicrobial peptides and their structure/function relationships, *Protein Pept. Lett. 12*, 31−39.
3. Brogden, K. A. (2005) Antimicrobial peptides: pore formers or metabolic inhibitors in bacteria?, *Nat. Rev. Microbiol. 3*, 238−250.
4. Powers, J. P., and Hancock, R. E. (2003) The relationship between peptide structure and antibacterial activity, *Peptides 24*, 1681−1691.
5. Dathe, M., and Wieprecht, T. (1999) Structural features of helical antimicrobial peptides: their potential to modulate activity on model membranes and biological cells, *Biochim. Biophys. Acta 1462*, 71−87.
6. Giangaspero, A., Sandri, L., and Tossi, A. (2001) Amphipathic alpha helical antimicrobial peptides, *Eur. J. Biochem. 268*, 5589−5600.
7. Sharadadevi, A., Sivakamasundari, C., and Nagaraj, R. (2005) Amphipathic alpha-helices in proteins: results from analysis of protein structures, *Proteins 59*, 791−801.
8. Efremov, R. G., and Vergoten, G. (1995) Hydrophobic nature of membrane-spanning α-helical peptides as revealed by Monte Carlo simulations and molecular hydrophobicity potential analysis, *J. Phys. Chem. 99*, 10658−10666.
9. Volynsky, P. E., Polyansky, A. A., Simakov, N. A., Arseniev, A. S., and Efremov, R. G. (2005) Effect of lipid composition on the "membrane response" induced by a fusion peptide, *Biochemistry 44*, 14626−14637.
10. Efremov, R. G., Volynsky, P. E., Nolde, D. E., Dubovskii, P. V., and Arseniev, A. S. (2002) Interaction of cardiotoxins with membranes: a molecular modeling study, *Biophys J. 83*, 144−153.
11. Pervushin, K. V., and Arseniev, A. S. (1995) NMR spectroscopy in the study of the spatial structure of membrane peptides and proteins, *Bioorg. Khim. 21*, 83−111.
12. Fernandez, C., and Wüthrich, K. (2003) NMR solution structure determination of membrane proteins reconstituted in detergent micelles, *FEBS Lett. 555*, 144−150.
13. Guba, W., Haessner, R., Breipohl, G., Henke, S., Knolle, J., Santagada, V., and Kessler, H. (1994) Combined approach of NMR and molecular dynamics within biphasic membrane mimetic: conformation and orientation of the bradykinin antagonist Hoe 140, *J. Am. Chem. Soc. 116*, 7532−7540.
14. Efremov, R. G., Nolde, D. E., Konshina, A. G., Syrtcev, N. P., and Arseniev, A. S. (2004) Peptides and proteins in membranes: what can we learn via computer simulations?, *Curr. Med. Chem. 11*, 2421−2442.
15. Oren, Z., and Shai, Y. (1998) Mode of action of linear amphipathic alpha-helical antimicrobial peptides, *Biopolymers 47*, 451−463.
16. Watts, A. (1998) Solid-state NMR approaches for studying the interaction of peptides and proteins with membranes, *Biochim. Biophys. Acta 1376*, 297−318.
17. Bechinger, B. (1999) The structure, dynamics and orientation of antimicrobial peptides in membranes by multidimensional solid-state NMR spectroscopy, *Biochim. Biophys. Acta 1462*, 157−183.
18. van Kan, E. J., Ganchev, D. N., Snel, M. M., Chupin, V., van der Bent, A., and de Kruijff B. (2003) The peptide antibiotic clavanin A interacts strongly and specifically with lipid bilayers, *Biochemistry 42*, 11366−11372.

19. Wang, G., Li, Y., and Li, X. (2005) Correlation of three-dimensional structures with the antibacterial activity of a group of peptides designed based on a nontoxic bacterial membrane anchor, *J. Biol. Chem. 280*, 5803−5811.
20. Mani, R., Waring, A. J., Lehrer, R. I., and Hong, M. (2005) Membrane-disruptive abilities of beta-hairpin antimicrobial peptides correlate with conformation and activity: a ^{31}P- and ^{1}H-NMR study, *Biochim. Biophys. Acta 1716*, 11−18.
21. Kozlov, S. A., Vassilevski, A. A., Feofanov, A. V., Surovoy, A. Yu., Karpunin, D. V., and Grishin, E. V. (2006) Latarcins: antimicrobial and cytolytic peptides from the venom of the spider *Lachesana tarabaevi* (Zodariidae) exemplify biomolecular diversity, *J. Biol. Chem. 281*, 20983−20992.
22. Murzyn, K., Rog, T., and Pasenkiewicz-Gierula, M. (2005) Phosphatidylethanolamine-phosphatidylglycerol bilayer as a model of the inner bacterial membrane, *Biophys. J. 88*, 1091−1103.
23. Dubovskii, P. V., Dementieva, D. V., Bocharov, E. V., Utkin, Y. N., and Arseniev, A. S. (2001) Membrane binding motif of the P-type cardiotoxin, *J. Mol. Biol. 305*, 137−149.
24. Dubovskii, P. V., Lesovoy, D. M., Dubinnyi, M. A., Utkin, Y. N., and Arseniev, A. S. (2003) Interaction of the P-type cardiotoxin with phospholipid membranes, *Eur. J. Biochem. 270*, 2038−2046.
25. Dubinnyi, M. A., Lesovoy, D. M., Dubovskii, P. V., Chupin, V. V., and Arseniev, A. S. (2006) Modeling of ^{31}P-NMR spectra of magnetically oriented phospholipid liposomes: a new analytical solution, *Solid State Nucl. Magn. Reson. 29*, 305−311.
26. Herrmann, T., Güntert, P., and Wüthrich, K. (2002) Protein NMR structure determination with automated NOE assignment using the new software CANDID and the torsion angle dynamics algorithm DYANA, *J. Mol. Biol. 319*, 209−227.
27. Güntert, P., Braun, W., and Wüthrich, K. (1991) Efficient computation of three-dimensional protein structures in solution from nuclear magnetic resonance data using the program DIANA and the supporting programs CALIBA, HABAS and GLOMSA, *J. Mol. Biol. 217*, 517−530.
28. Koradi, R., Billeter, M., and Wüthrich, K. (1996) MOLMOL: a program for display and analysis of macromolecular structures, *J. Mol. Graphics 14*, 51−55.
29. Morris, L. A., MacArthur, M. W., Hutchinson, E. G., and Thornton, J. M. (1992) Stereochemical quality of protein structure coordinates, *Proteins 12*, 345−364.
30. Laskowski, R. A., MacArthur, M. W., Moss, D. S., and Thornton, J. M. (1993) PROCHECK: a program to check the stereochemical quality of protein structures, *J. Appl. Crystallogr. 26*, 283−291.
31. Nolde, D. E., Arseniev, A. S., Vergoten, G., and Efremov, R. G. (1997) Atomic solvation parameters for proteins in a membrane environment. Application to transmembrane α-helices, *J. Biomol. Struct., Dyn. 15*, 1−18.
32. von Freyberg, B., and Braun, W. (1991) Efficient search for all low energy conformations of polypeptides by Monte Carlo methods, *J. Comput. Chem. 12*, 1065−1076.
33. Dubovskii, P. V., Li, H., Takahashi, S., Arseniev, A. S., and Akasaka, K. (2000) Structure of an analog of fusion peptide from hemagglutinin, *Protein Sci. 9*, 786−798.
34. Papavoine, C. H., Konings, R. N., Hilbers, C. W., and van de Ven, F. J. (1994) Location of M13 coat protein in sodium dodecyl sulfate micelles as determined by NMR, *Biochemistry 33*, 12990−12997.
35. Wüthrich, K. (1986) *NMR of Proteins and Nucleic Acids*, Wiley, New York.
36. Szilágyi, L., and Jardetzky, O. (1989) α-Proton chemical shifts and secondary structure in proteins, *J. Magn. Reson. 83*, 441−449.
37. Wishart, D. S., Sykes, B. D., and Richards, F. M. (1991) Relationship between nuclear magnetic resonance chemical shift and protein secondary structure, *J. Mol. Biol. 222*, 311−333.
38. Burnell, E. E., Cullis, P. R., and de Kruijff, B. (1980) Effects of tumbling and lateral diffusion on phosphatidylcholine model membrane ^{31}P-NMR lineshapes, *Biochim. Biophys. Acta 603*, 63−69.
39. Shin, K., Maeda, H., Fujiwara, T., and Akutsu, H. (1995) Molecular miscibility of phosphatidylcholine and phosphatidylethanolamine in binary mixed bilayers with acidic phospholipids studied by ^{2}H- and ^{31}P-NMR, *Biochim. Biophys. Acta 1238*, 42−48.
40. Rizo, J., Blanco, F. J., Kobe, B., Bruch, M. D., and Gierasch, L. M. (1993) Conformational behavior of *Escherichia coli* OmpA signal peptides in membrane mimetic environments, *Biochemistry 32*, 4881−4894.
41. Han, X., Bushweller, J. H., Cafiso, D. S., and Tamm, L. K. (2001) Membrane structure and fusion-triggering conformational change of the fusion domain from influenza hemagglutinin, *Nat. Struct. Biol. 8*, 715−720.
42. Oh, D., Shin, S. Y., Lee, S., Kang, J. H., Kim, S. D., Ryu, P. D., Hahm, K. S., and Kim, Y. (2000) Role of the hinge region and the tryptophan residue in the synthetic antimicrobial peptides, cecropin A(1−8)-magainin 2(1−12) and its analogues, on their antibiotic activities and structures, *Biochemistry 39*, 11855−11864.
43. Pukala, T. L., Brinkworth, C. S., Carver, J. A., and Bowie, J. H. (2004) Investigating the importance of the flexible hinge in caerin 1.1: solution structures and activity of two synthetically modified caerin peptides, *Biochemistry 43*, 937−944.
44. van Kan, E. J., van der Bent, A., Demel, R. A., and de Kruijff, B. (2001) Membrane activity of the peptide antibiotic clavanin and the importance of its glycine residues, *Biochemistry 40*, 6398−6405.
45. Seelig, J., Macdonald, P. M., and Scherer, P. G. (1987) Phospholipid head groups as sensors of electric charge in membranes, *Biochemistry 26*, 7535−7541.
46. Ramamoorthy, A., Thennarasu, S., Tan, A., Gottipati, K., Sreekumar, S., Heyl, D. L., An, F. Y., and Shelburne, C. E. (2006) Deletion of all cysteines in tachyplesin I abolishes hemolytic activity and retains antimicrobial activity and lipopolysaccharide selective binding, *Biochemistry 45*, 6529−6540.
47. Lu, J. X., Damodaran, K., Blazyk, J., and Lorigan, G. A. (2005) Solid-state nuclear magnetic resonance relaxation studies of the interaction mechanism of antimicrobial peptides with phospholipid bilayer membranes, *Biochemistry 44*, 10208−10217.
48. Poklar, N., Fritz, J., Macek, P., Vesnaver, G., and Chalikian, T. V. (1999) Interaction of the pore-forming protein equinatoxin II with model lipid membranes: a calorimetric and spectroscopic study, *Biochemistry 38*, 14999−15008.
49. Mani, R., Buffy, J. J., Waring, A. J., Lehrer, R. I., and Hong, M. (2004) Solid-state NMR investigation of the selective disruption of lipid membranes by protegrin-1, *Biochemistry 43*, 13839−13848.
50. Wang, Z., and Wang, G. (2004) APD: the antimicrobial peptide database, *Nucleic Acids Res. 32*, D590−D592.
51. Strahilevitz, J., Mor, A., Nicolas, P., and Shai, Y. (1994) Spectrum of antimicrobial activity and assembly of dermaseptin B and its precursor form in phospholipid membranes, *Biochemistry 33*, 10951−10960.
52. Brasseur, R., Pillot, T., Lins, L., Vandekerckhove, J., and Rosseneu, M. (1997) Peptides in membranes: tipping the balance of membrane stability, *Trends Biochem. Sci. 22*, 167−171.
53. Efremov, R. G., Nolde, D. E., Volynsky, P. E., Chernyavsky, A. A., Dubovskii, P. V., and Arseniev, A. S. (1999) Factors important for fusogenic activity of peptides: molecular modeling study of analogs of fusion peptide of influenza virus hemagglutinin, *FEBS Lett. 462*, 205−210.
54. Lequin, O., Bruston, F., Convert, O., Chassaing, G., and Nicolas, P. (2003) Helical structure of dermaseptin B2 in a membrane-mimetic environment, *Biochemistry 42*, 10311−10323.
55. Tieleman, P., Shrivastava, I. H., Ulmschneider, M. R., and Sansom, M. S. P. (2001) Proline-induced hinges in transmembrane helices: possible roles in ion channel gating, *Proteins: Struct., Funct., Genet. 44*, 63−72.

BI060635W